Falkland Island Fisheries Department

Loligo gahi Stock Assessment, First Season 2011

Andreas Winter

May 2011

Index

Summary

1) The first season *Loligo* fishery of 2011 was open for 50 days, from February 24 to April 14. 15,271 tonnes of *Loligo* catch were reported; significantly lower than first season 2010 but higher than first season 2009. 56.6% of *Loligo* catch and 55.4% of effort were taken north of 52º S.
2) The sub-area north of 52º S was closed from midnight March 23 until midnight March 31 following early indications that the *Loligo* stock was starting to deplete. *Illex* were present in the north sub-area, causing predation on *Loligo* and causing some C-licence fishing effort to be diverted from *Loligo* to *Illex*.
3) The fishing fleet alternated strongly between sub-areas, with most vessels concentrated either north or south at any one time. North and south sub-areas were therefore depletion-modelled separately.
4) Depletion periods north were inferred to have started on March 6 and April 6. Depletion periods south were inferred to have started on March 25 and April 1. CPUE trends and *Loligo* size data suggested that further immigrations / depletions may have started in the final few days of the season, but these could no longer be modelled from the in-season data.
5) In-season immigration was estimated at 10,415 ± 6,892 tonnes. Combined with the pre-season estimate of 16,095 ± 8,263 tonnes, a total of 26,510 ± 10,760 tonnes of *Loligo* were present in the Falkland Islands fishing zone during the first season of 2011.
6) The final total estimate for *Loligo* remaining in the *Loligo* Box at the end of the season was:

   Maximum likelihood of 9,115 tonnes, with 95% confidence interval of [5,735 to 16,026] tonnes.

   The risk of *Loligo* escapement biomass at the end of the season being less than 10,000 tonnes was estimated at 53.5%.

Introduction

The first season of the 2011 *Loligo gahi* squid fishery started on February 24, and ended by directed closure on April 14. Total reported *Loligo* catch by C-licensed vessels was 15,271 tonnes, which is little more than half the total of the 2010 first season (28,754 tonnes; Winter, 2010a), but higher than the total of the 2009 first season (12,764 tonnes; Payá, 2009).

The 2011 first season *Loligo* fishery was characterized by a high abundance of shortfin squid *Illex argentinus* in the northern part of the *Loligo* Box. Compared with the previous year, warmer water penetrated further from the Patagonian Shelf to the northeastern Falkland Shelf (Figure 1), facilitating the influx of *Illex argentinus* which is a temperate species (Haimovici et al., 1998). Arkhipkin and Middleton (2002a) concluded that *Illex* may interact by predation or competition with *Loligo* in years when their ranges overlap. During the 2011 first *Loligo* season, *Illex* specimens sampled at sea were found to have consumed large numbers of *Loligo*. Furthermore, since *Illex* is itself a commercially important squid (Barton, 2002, Harte and Barton, 2007), the high abundance of *Illex* influenced operations of the *Loligo* fishery by motivating some C-licence holders to temporarily target *Illex*.

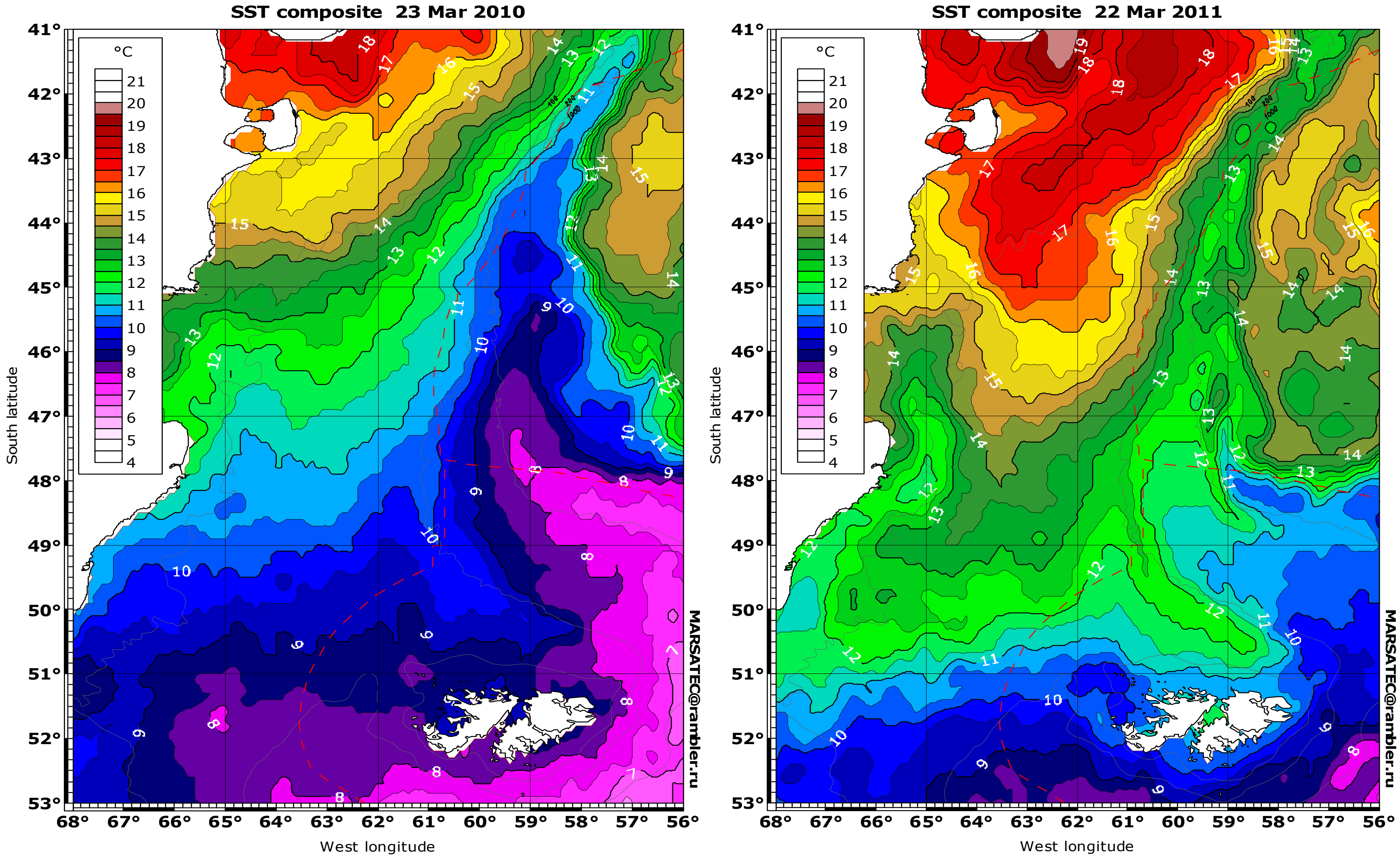

Figure 1. Satellite composite sea surface temperatures, comparing 23 March 2010 and 22 March 2011.

As in previous seasons, the *Loligo* stock assessment was conducted with a depletion model (Agnew et al., 1998; Roa-Ureta and Arkhipkin, 2007; Arkhipkin et al., 2008). Because *Loligo* has an annual life cycle (Patterson, 1988), stock cannot be derived from a standing biomass carried over from prior years (Rosenberg et al., 1990). The depletion model instead back-calculates an estimate of initial abundance from data on catch, effort, and natural mortality (Roa-Ureta and Arkhipkin, 2007). In its basic form (DeLury, 1947) the depletion model assumes a closed population in a fixed area for the duration of the assessment. This assumption is imperfectly met in the Falkland Islands fishery, where stock analyses have often shown that *Loligo* groups arrive in successive waves after the start of the season (Payá, 2009; 2010; Winter, 2010a). Successive arrivals are revealed by discontinuities in the data. Fishing on a single, closed cohort would be expected to yield gradually decreasing CPUE, but gradually increasing average squid sizes. When instead these measures change suddenly, or in contrast to expectation, then the arrival of a new group may be inferred. In this event, the new group arrival/depletion is parameterized and modelled separately. Squid from preceding groups that are still alive at the next arrival are included in the next model, as there is no practical way to distinguish them in the fishery. Ultimately, the most important depletion model is that of the last group, since this will determine whether the escapement biomass limit of 10,000 tonnes (Barton, 2002) has been fulfilled.

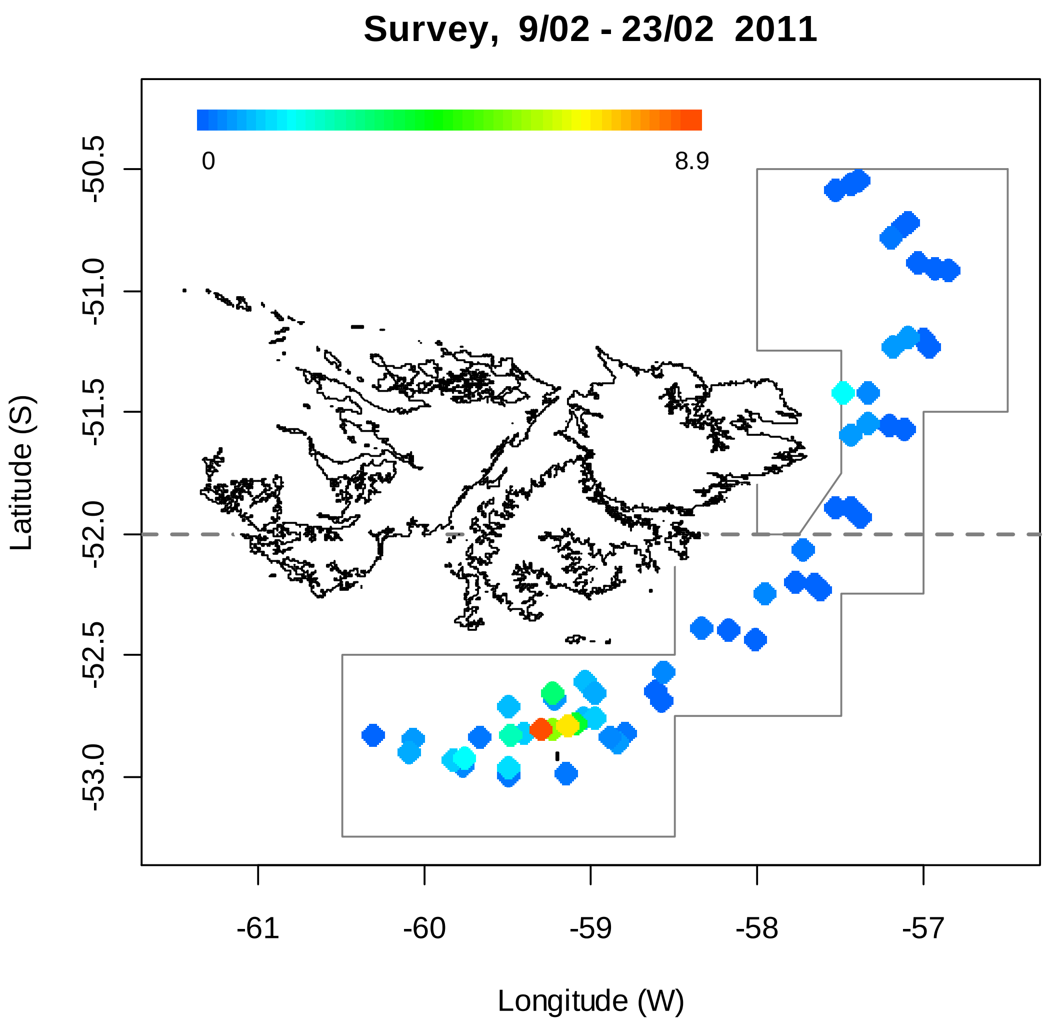

Figure 2 [previous page]. Spatial distribution of *Loligo* 1st-season pre-season survey catches, scaled to catch weight (maximum = 8.9 tonnes). Fifty-nine catches are represented. The '*Loligo* Box' fishing zone, as well as the 52 ºS parallel delineating the nominal boundary between north and south assessment areas, are shown in gray.

Figure 3 [below]. Spatial distribution of *Loligo* 1st-season commercial catches, scaled to catch weight (maximum = 26.4 tonnes). 2395 catches were taken during the season. The '*Loligo* Box' fishing zone, as well as the 52 ºS parallel delineating the nominal boundary between north and south assessment areas, are shown in gray.

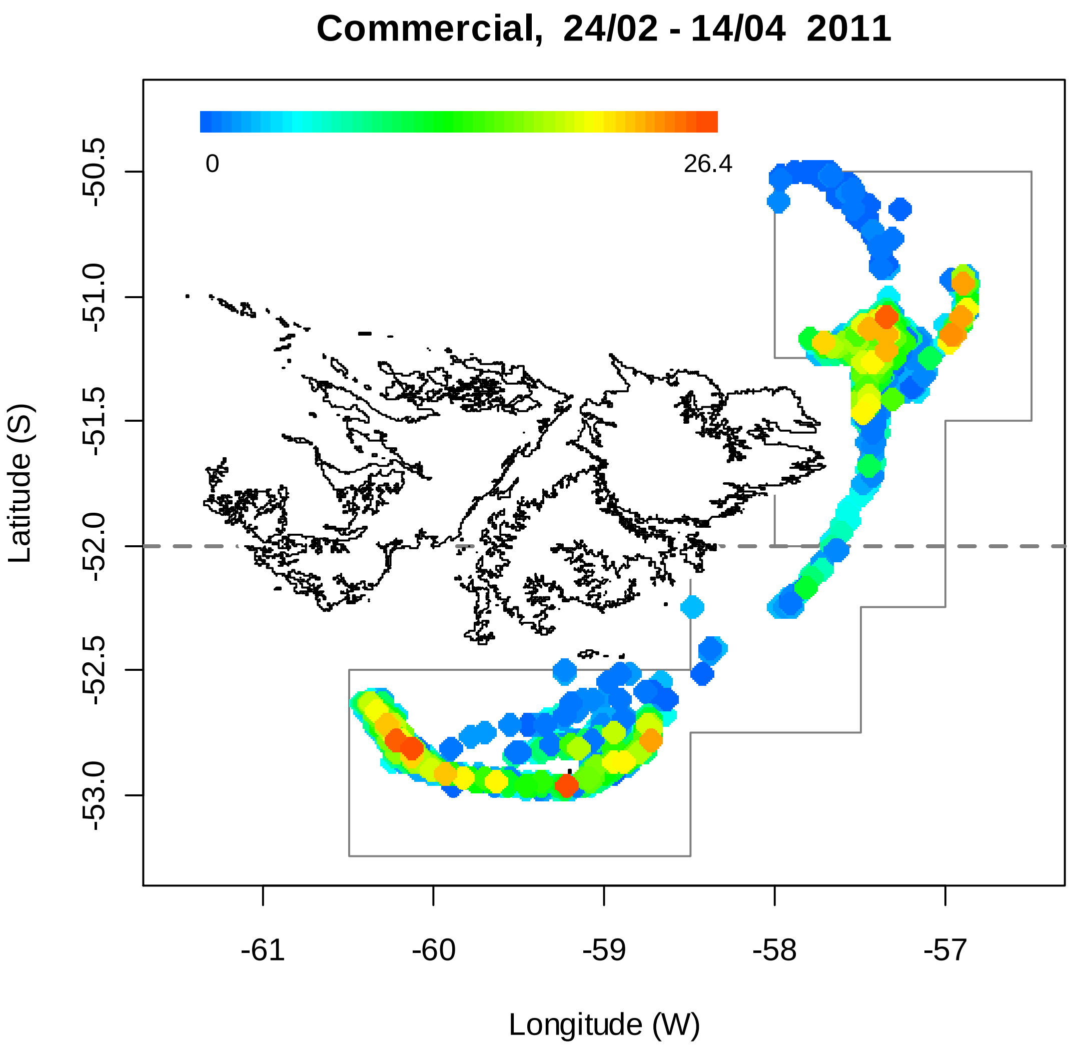

The stock assessment was performed in a Bayesian framework (Punt and Hilborn, 1997), whereby results of the depletion model are conditioned by prior information on the stock. Distributions of the stock estimates (i.e., measures of their statistical uncertainty) were then computed using a Markov Chain Monte Carlo (MCMC) with Metropolis-Hastings algorithm (Gamerman and Lopes, 2006). MCMC is an iterative method which generates random stepwise changes to the proposed outcome of a model (in this case, the number of

Loligo) and at each step, accepts or nullifies the change with a probability equivalent to how well the change fits the model parameters compared to the previous step. The resulting sequence of accepted or nullified changes (i.e., the 'chain') approximates the probability distribution of the model outcome. This approximation is useful for models such as depletion, which have probability distributions that are difficult to sample directly.

Stock assessment
Data

The 2011 first preseason survey had caught 66.76 tonnes *Loligo* in the fishing area, with two zones of modest concentration north and south in the *Loligo* Box (Winter et al., 2011; Figure 2). Commercial catches in-season showed a similar distribution of catch concentrations (Figure 3). The 52 ºS latitude was again used as a nominal boundary between north (North-Central) and south (Beauchêne) assessment sub-areas. Over the entire season, 56.6% of *Loligo* catch and 55.4% of effort (vessel-days) were taken north of 52 ºS, vs. 43.4% of catch and 44.6% of effort south of 52 ºS. This represents the only first season since at least 2005 in which less than 50% of *Loligo* catch was taken in the Beauchêne sub-area.

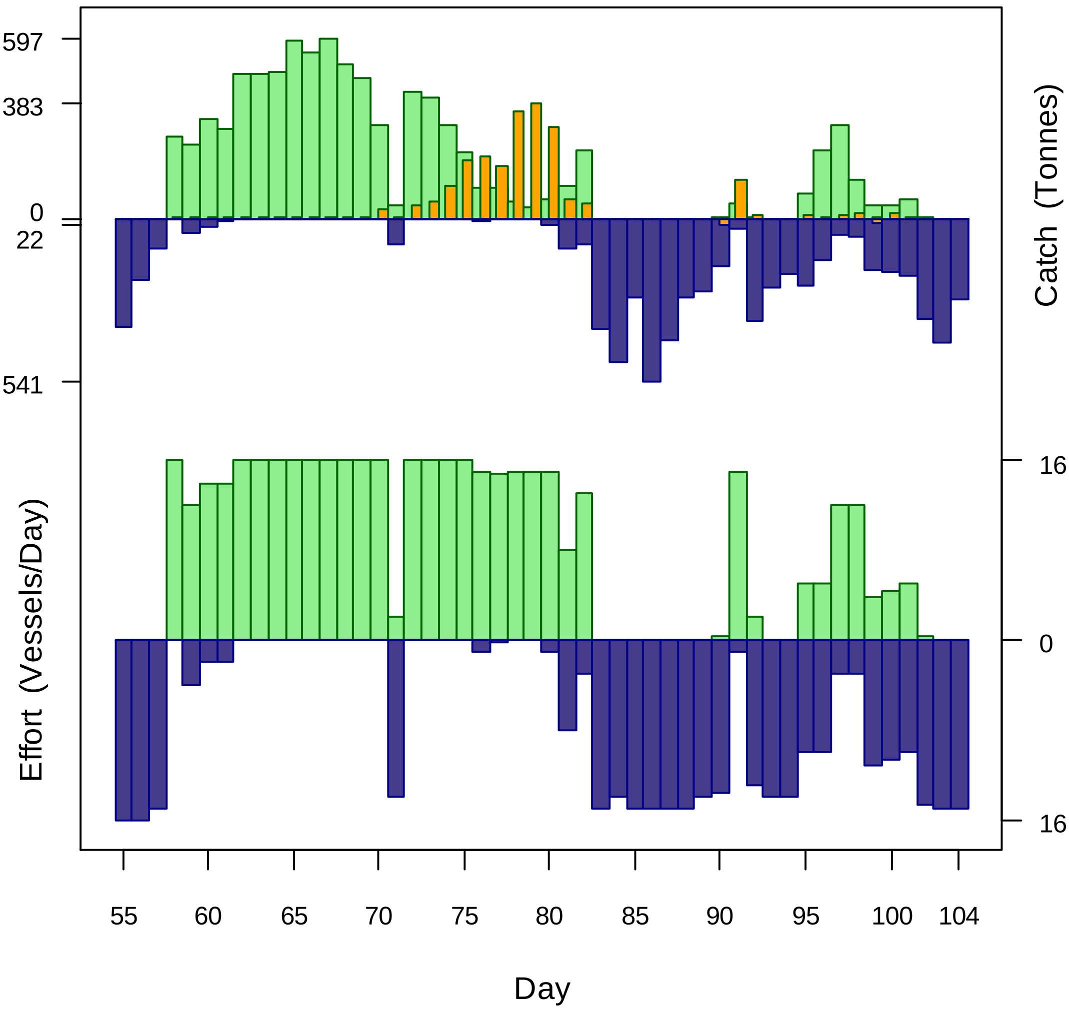

Figure 4 [previous page]. Daily total *Loligo* catch and effort distribution by assessment sub-area north (green) and south (purple) of the 52º S parallel in the *Loligo* 1st season 2011. The season was opened from February 24 (chronological day 55) to April 14 (chronological day 104). As many as 16 vessels fished per day north of 52º S; as many as 16 vessels fished per day south of 52º S. As much as 597 tonnes *Loligo* were caught per day north of 52º S; as much as 541 tonnes *Loligo* were caught per day south of 52º S. Additionally, as much as 383 tonnes *Illex* (orange) were caught per day north of 52º S; as much as 22 tonnes *Illex* were caught per day south of 52º S.

Between 14 and 16 vessels fished in the commercial season on any day, for a total of 770 vessel-days. These vessels reported daily catch totals to the FIFD and electronic logbook data that included trawl times, positions, and product weight by market size categories. Two FIFD observers were deployed on three vessels in the fishery for a total of 50 observer-days. Throughout the 50 days of the season, 48 days had 1 observer covering, 1 day had two observers, and 1 day had no observers. Each observer sampled an average of 416 *Loligo* daily, and reported their maturity stages, sex, and lengths to 0.5 cm.

Catches of *Illex* surpassed catches of *Loligo* in the north on five days between March 17 and March 21 (day 76 to day 80) (Figure 4). At that time, *Loligo* in the north showed signs of significant depletion. As a result, the Director of Natural Resources ordered fishing in the *Loligo* Box north of 52 ºS stopped from midnight March 23 until midnight March 31.

Group arrivals / depletion curves

Loligo fishing in the first season 2011 tended to alternate strongly between sub-areas. Although total effort was split 55.4% north / 44.6% south, only seven of the 50 season-days had less than 80% of the fleet concentrated either north or south at one time (Figure 4), which albeit was partly imposed by the 8-day closure of the north (noted above). From previous studies, units of the *Loligo* stock in different sub-areas are known to have different movement patterns (Arkhipkin and Middleton, 2002b; Arkhipkin et al., 2004a; 2004b). Depletion curves were therefore calculated by north and south sub-areas separately.

Start and end days of depletions - following arrivals of new *Loligo* groups - were judged from daily changes in CPUE, *Loligo* sex proportions, and average individual *Loligo* sizes. CPUE was calculated as metric tonnes of *Loligo* caught per vessel per day. Days were used rather than trawl hours as the basic unit of effort, to more consistently represent vessels' overall fishing power, which is a factor of processing capacity as well as trawling capacity. Effort-days were also adjusted to reflect that vessels were sometimes targeting *Illex*, and therefore not effectively expending the effort on *Loligo*. The adjustment consisted of setting a fractional value for a vessel 'effort-day' equivalent to the ratio between *Loligo* and *Illex* catch for that vessel's day, with two conditions: total catch was at least 10 tonnes and *Illex* catch was at least 10% of *Loligo* catch. For example, if a vessel on one day caught 18.3 t *Loligo* and 13.5 t *Illex*, its effort-day value with respect to *Loligo* CPUE would be considered 0.58 rather than 1.

Average individual *Loligo* sizes were expressed as weight (kg), converted from mantle lengths using Roa-Ureta and Arkhipkin's (2007) formula with combined data from 2006 and 2007:

$$weight(kg) = 0.32411926 \times length(cm)^{1.97547877} \times 1000^{-1} \qquad \textbf{(1)}$$

Mantle lengths were obtained from in-season observer data, and also from in-season commercial data as the proportion of product weight that vessels reported per market size category (Payá, 2006). Observer mantle lengths are scientifically precise, but restricted to 1-2 vessels at any one time that may or may not be representative of the entire fleet. Commercially proportioned mantle lengths are relatively imprecise, but cover the entire fishing fleet. Therefore, both sources of data were examined.

Depletion period selection

The *Loligo* data and CPUE time series showed two days in the north and two days in the south that plausibly represent the onset of separate depletions (Figures 5 and 6). None coincided with the actual start of the season; *Loligo* seasons have often shown a lag phase before depletion (Payá, 2010, Winter, 2010a; 2010b), during which time initial dense aggregations of the standing stock are 'fished-up'.

- The first depletion north was identified on day 65, seven days after fishing started in the north. CPUE reached a first significant peak (Figure 5) while average individual weights from both observer data (Figure 6A) and commercial data (Figure 6B) showed a slight local minimum.
- The second depletion north was identified on day 96, five days after *Loligo* fishing was re-opened in the north. CPUE and average individual weight from commercial data both peaked sharply (Figures 5 and 6B).
- The first depletion south was identified on day 84, with a first significant peak in CPUE (Figure 5), the onset of a declining trend in proportion of females (Figure 6C), and a noticeable discontinuity in average individual weight from observer data (Figure 6A) (although day 84 itself happened to be the one day with no observer coverage).
- The second depletion south was identified on day 91. CPUE was at its highest peak (Figure 5), and proportion of females decreased the day after, having increased for three days straight the day before (Figure 6C).

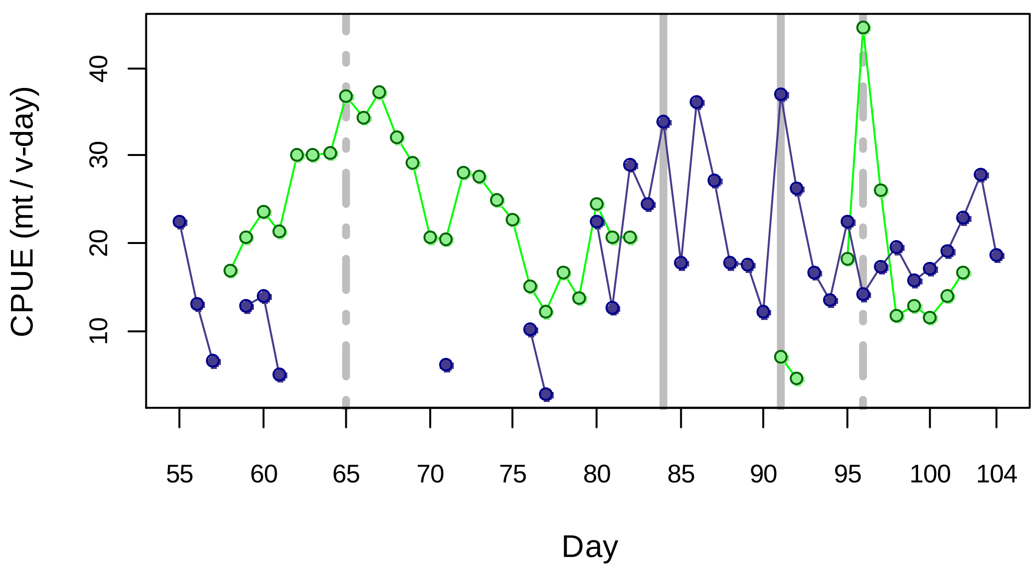

Figure 5. CPUE in metric tonnes per vessel per day, by assessment sub-area north (green) and south (purple) of the 52º S parallel. Data from consecutive days are joined by line segments. Broken gray vertical bars indicate days that were identified as the onset of depletions north: days 65 and 96. Solid gray vertical bars indicate days that were identified as the onset of depletions south: days 84 and 91.

A

B

C

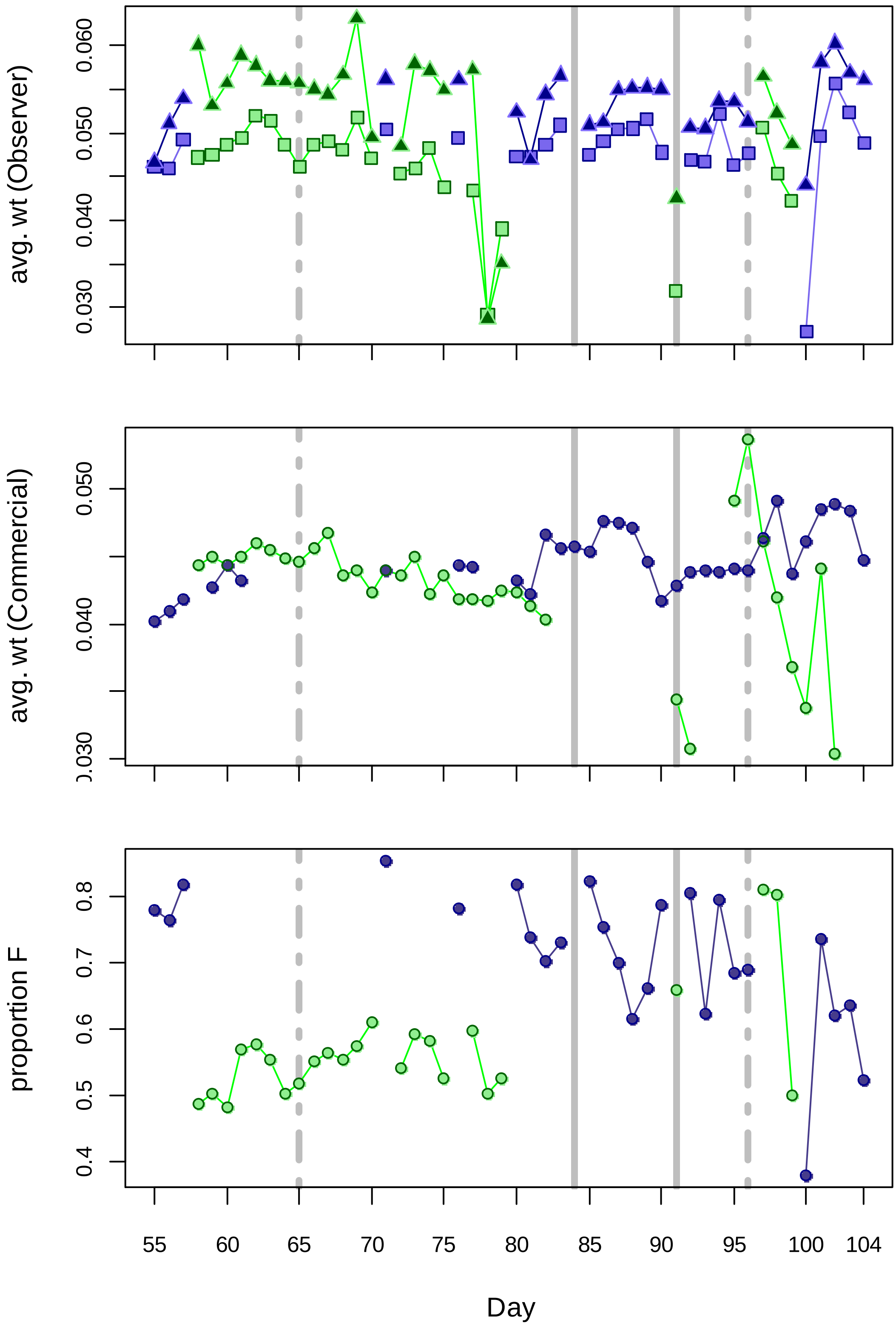

Figure 6. **A**: Average individual *Loligo* weights (kg) by sex per day from observer sampling. Male: triangles, female: squares. **B**: Average individual *Loligo* weights (kg) per day from commercial size categories. **C**: Proportions of female *Loligo* per day from observer sampling. All other plot symbols and colours as in Figure 5.

Depletion model and prior

The formulation of the Bayesian assessment model has been described previously (e.g., Payá, 2009). For the first season 2011 assessment, probability density function of the prior, and log-likelihood of the depletion curve, were assumed to follow a Gaussian distribution. But unlike previous seasons (Payá, 2010, Winter, 2010a; 2010b), likelihood calculations of the depletion curves were no longer optimized over individual vessel differences in catchability, which has been found to over-parameterize the assessment model. Three chains of the MCMC were computed for each model. One chain was started at the estimated optimum *Loligo* number (i.e., the chain was started about where it was expected to end), one chain was started at a low underestimate, and one chain was started at a high overestimate, to check that the algorithm did converge. Chains were run for 30,000 iterations; the first 3,000 iterations were discarded as burn-in sections (initial phases over which the algorithm stabilizes), then thinned by a factor of three to reduce serial correlation (only every third iteration was retained). Convergence of the three chains was accepted if the variance among chains was less than 10% higher than the variance within chains (Brooks and Gelman, 1998). When convergence was satisfied the three chains were combined as one set of 27,000 samples.

The Bayesian prior for depletion at the start of the season was based on the pre-season survey estimate for total *Loligo* biomass. This estimate had been calculated at 16,095 ± 4722 tonnes (Winter et al., 2011). Based on acoustic data analyses, Payá (2010) and Winter (2010a) estimated a net escapement of up to 22%, which was added to the standard deviation:

$$16{,}095 \pm \left(\frac{4722}{16{,}095} + .220\right) \;=\; 16{,}095 \,\pm\, 51.3\% \;=\; 16{,}095 \,\pm\, 8263 \text{ tonnes.} \qquad \textbf{(2)}$$

The 22% was added as a linear increase in the variability, but was not used to reduce the total estimate, because *Loligo* that escape one trawl are likely to be part of the biomass concentration that is available to the next trawl. This estimate in biomass was converted to an estimate in numbers using the size-frequency distributions sampled during the pre-season survey (Winter et al., 2011).

Loligo were sampled at 52 pre-season survey stations, giving a geospatially-averaged (both sexes) mantle length of 12.29 cm, with coefficients of variation of 4.68% from the geospatial model and 0.4% from random variation of the length-frequency sampling; estimated by bootstrapping (Efron, 1981). The mantle length of 12.29 cm corresponds to 0.046 kg individual weight (equation 1), and combining the average weight calculations with equation 2 thus gave estimated *Loligo* numbers, with error distribution, at the end of the survey / start of the season (Feb. 24; day 55) of:

$$N_{\text{day }55} = \frac{16{,}095 \times 1000}{0.046} \pm \sqrt{51.3\%^2 + 4.7\%^2 + 0.4\%^2}$$

$$= 0.350 \times 10^9 \pm 51.6\% = 0.350 \times 10^9 \pm 0.180 \times 10^9 \qquad \textbf{(3)}$$

which was split between north and south of 52 ºS as:

$$N_{N\text{ day }55} = 0.153 \times 10^9 \pm 0.119 \times 10^9 \qquad \textbf{(3N)}$$
$$N_{S\text{ day }55} = 0.197 \times 10^9 \pm 0.092 \times 10^9 \qquad \textbf{(3S)}$$

With depletion starting on day x after the start of the season (day 55), *Loligo* numbers at the start of depletion are discounted for both catch and estimated natural mortality occurring during the intervening days:

$$_{\text{prior}}\,N_{\text{day }x} \quad = \quad N_{\text{day }55} \times e^{-M\,(\text{day }x\,-\,\text{day }55)} - CNMD_{\text{day }x} \qquad \textbf{(4)}$$

where CNMD is the cumulative catch in numbers discounted for the proportion that would have died naturally anyway over the period of time:

$$CNMD_{\text{start day}} \quad = \quad 0$$
$$CNMD_{\text{day }x} \quad = \quad CNMD_{\text{day }x-1} \times e^{-M} + C_{n\text{ day }x-1} \times e^{-M/2} \qquad \textbf{(5)}$$

Natural mortality M is considered constant at 0.0133 day^{-1} (Roa-Ureta and Arkhipkin, 2007). C_n is the daily catch total in numbers. This is calculated as the daily reported *Loligo* catch tonnage divided by the day's average individual weight. Days' average individual weights were calculated by averaging observer size samples and commercial size categories where observer data were available, otherwise only commercial size categories. The $_{\text{prior}}\,N_{\text{day }x}$ (equation 4) may in some cases need to be overridden to ensure that a minimum number of *Loligo* (nominally: two) will be left at the end of the depletion period (i.e., the number of *Loligo* cannot go extinct or go negative). For depletion ending day y this $_{\text{prior}}$ N minimum is calculated as:

$$_{\text{prior}}\,N_{\text{min day }x} \quad = \quad 2 + \frac{CNMD_{\text{day y}}}{e^{(-M\,(\text{day y - day x}))}} \qquad \textbf{(6)}$$

For subsequent arrival / depletions during the season, the Bayesian prior could not be based on the pre-season survey, since it was assumed that the subsequent depletions involve different groups of *Loligo*. Instead, it was inferred that the ratio of *Loligo* numbers on a subsequent depletion start day, over the *Loligo* numbers on the day before, should be proportional to the ratio of CPUE on those two days. *Loligo* numbers on the day before were calculated by setting day x in equations (4, 5) as the 'day before', and replacing day 55 in equation 4 with start day of the previous depletion period. CPUE were calculated as the aggregate CPUE of all vessels fishing on either day in the north or south sub-area being modelled. Because CPUE represents biomass, the prior estimate from this ratio was also scaled by the proportional increase or decrease of *Loligo* average individual weight on those two days. Error distribution of this prior estimate was summed from three components: variability of the 'day before' abundance estimate, calculated as the MCMC coefficient of variation of the depletion to which the 'day before' belonged, variability of the CPUE ratio, calculated by bootstrap re-sampling 10000× the vessels fishing on either day, and variability in the proportional change of average individual weight, calculated as the coefficient of variation in day-to-day differences in average individual weight during the depletion.

In-season depletion is modelled by the same basic algorithm as equations 4 and 5. However in this case, there is no extrinsic estimate (e.g., from a survey) for the starting-day count (equivalent to $N_{\text{day }55}$ in equation 4). Instead, the algorithm is solved by minimizing the difference function between actual observed catches on each day i of the depletion period, and predicted catches on each day i according to:

$$_{\text{predicted}}\,C_{n\text{ day }i} \quad = \quad q_{\text{avg}} \times \text{effort}_{\text{ day }i} \times {}_{\text{predicted}}\,N_{\text{ day }i} \times e^{-M/2} \qquad \textbf{(7)}$$

where

$$_{\text{predicted}} N_{\text{day } i} = N_{\text{day } start} \times e^{-M \times (\text{day } i - \text{day } start)} - CNMD_{\text{day } i}, \qquad \text{as before.}$$

The difference function

$$\sigma = \sqrt{\overline{\left(\log(\text{predicted } C_n) - \log(\text{actual } C_n)\right)^2}\Big|_i}$$

is minimized in the Gaussian form: **(8)**

$$\text{depletion llhood} = \sum_i -\log\left(\frac{1}{\sqrt{2\pi\sigma^2}} \times \exp\left(\frac{(\log(\text{pred.}C_{ni}) - \log(\text{act.}C_{ni}))^2}{2\sigma^2}\right)\right)$$

$N_{\text{day } start}$ and q_{avg} are the free parameters in the minimization; q_{avg} is the average catchability coefficient (Arreguin-Sanchez, 1996) for the fishing vessels over that depletion period. The trend of predicted catch numbers per day can then be plotted comparatively with actual catch numbers per day to evaluate model fit with respect to each depletion period (Figures 7, 8).

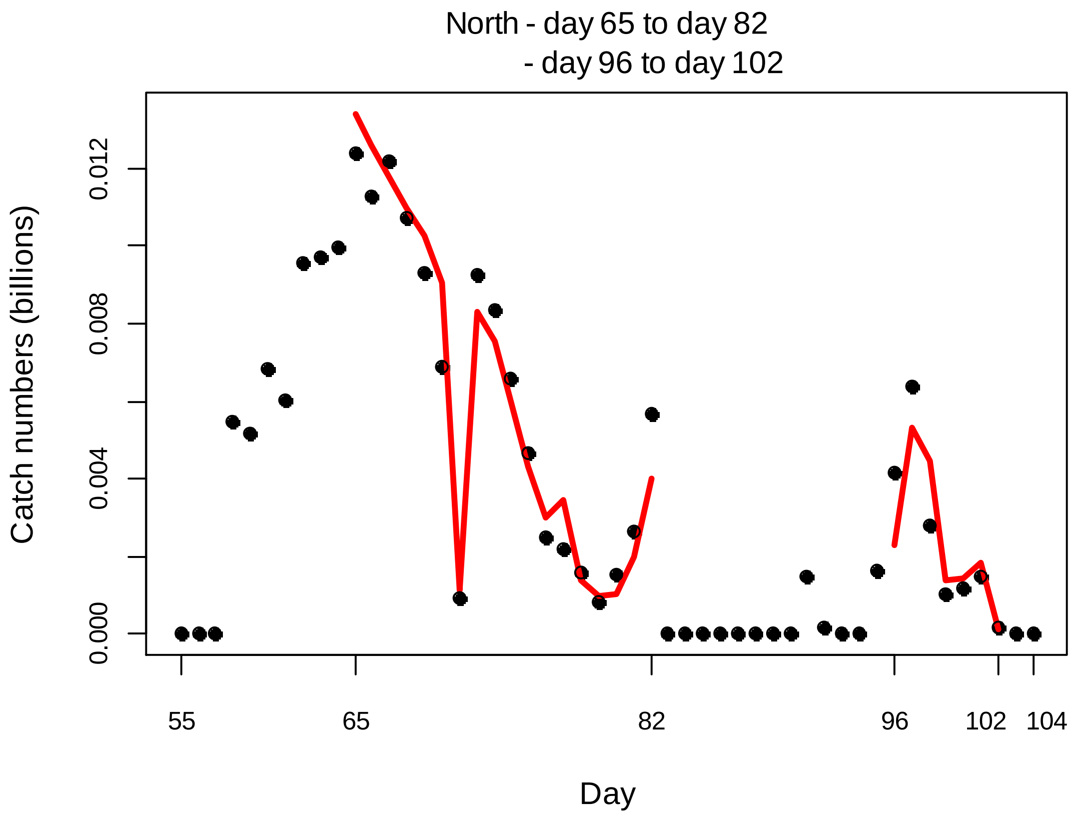

Figure 7. Daily estimated catch numbers (black points) and expected catch numbers (red lines) projected from the north sub-area depletions, starting on days 65 and 96.

Figure 8 [next page]. Daily estimated catch numbers (black points) and expected catch numbers (red lines) projected from the south sub-area depletions, starting on days 84 and 91.

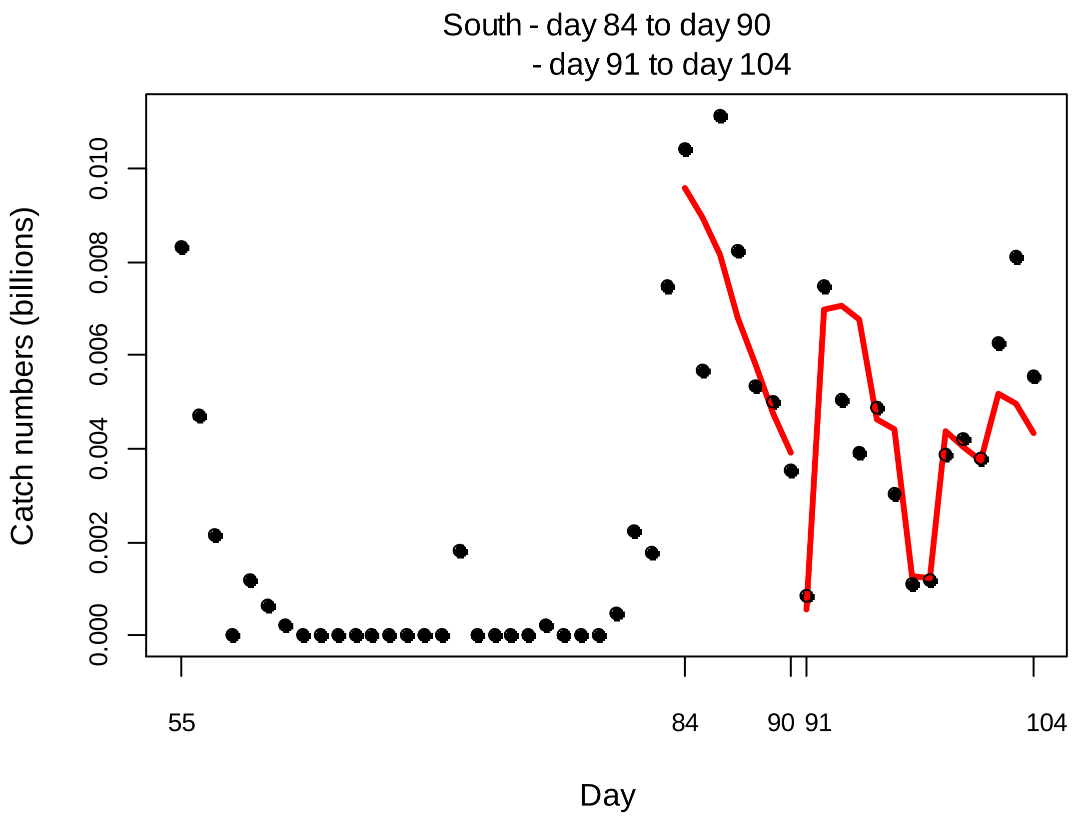

Depletion analyses
First depletion north

For the first depletion north assumed to start on day 65, the estimated prior for initial abundance, using equations (3N, 4, 5), was:

$$\begin{aligned} CNMD_{N\ day\ 65} &= 0.051 \times 10^9 \\ {}_{prior}\,N_{N\ day\ 65} &= 0.153 \times 10^9 \times e^{-0.0133 \times (65-55)} - CNMD_{N\ day\ 65} \\ &= 0.083 \times 10^9 \end{aligned}$$

However, in this case the $_{prior}$ N minimum (cf. equation 6) was higher at:

$$_{prior}N_{N\ min\ day\ 65} = 2 + \frac{0.089 \times 10^9}{e^{(-M\,(82-65))}} = 0.112 \times 10^9, \qquad \textbf{(9)}$$

and was therefore retained as the prior N (with the same standard error; not shown). This estimate was input to the analysis, and is equivalent to the maximum of the prior likelihood distribution (Figure 9, red line). The maximum likelihood of the depletion model, using equations (7, 8) was found at $_{depletion}N_{N\ day\ 65} = 0.247 \times 10^9$ (Figure 9, blue line). This depletion model predominantly controlled the distribution of the posterior (Figure 9, gray bars). It is notable that the prior distribution, derived from the survey, strongly underrated *Loligo* abundance in the north, supporting the hypothesis that by the end of the survey *Loligo* had not fully immigrated to the fishing area (Winter et al., 2011).

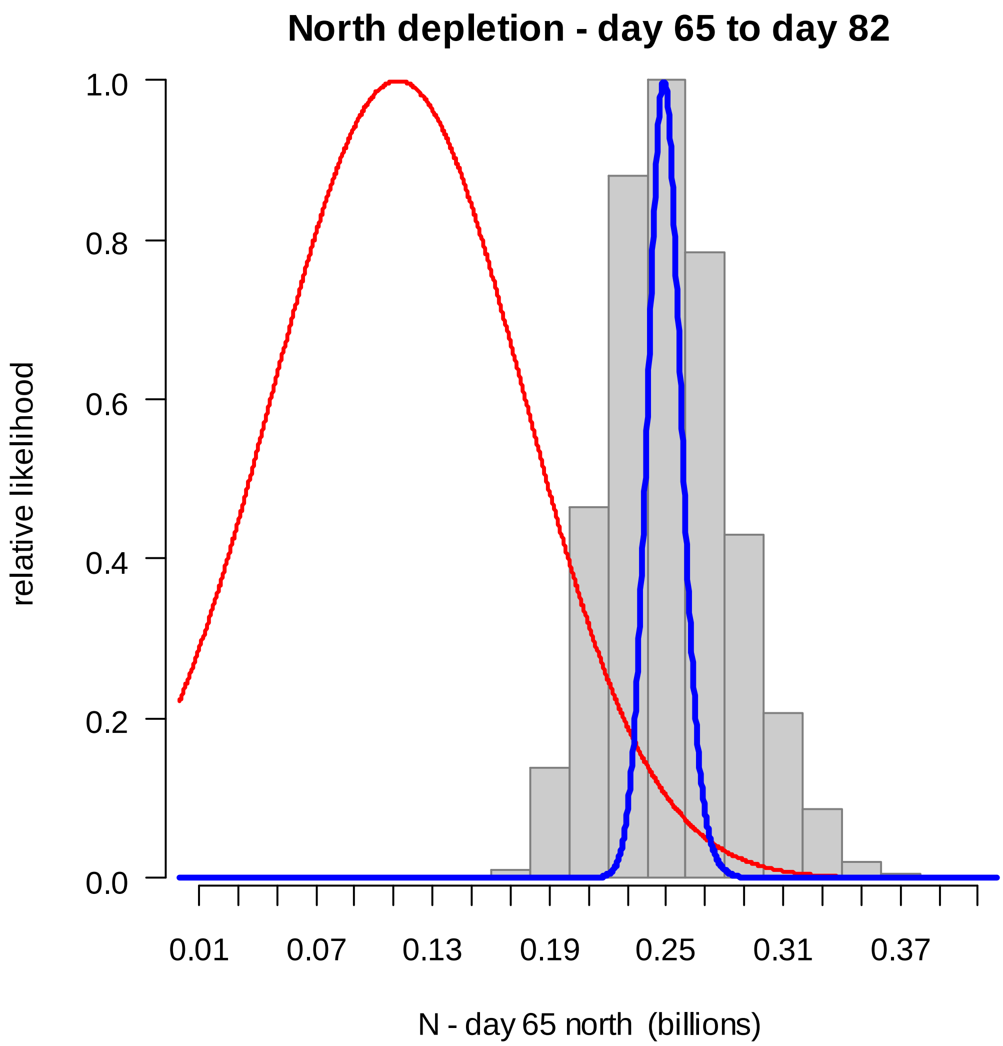

Figure 9. Model likelihood distributions for N billion *Loligo* present in the north sub-area fishery on day 65 (March 6). Red line: prior model (derived from pre-season survey data), blue line: depletion model from day 65 to day 82, gray bars: posterior.

Second depletion north

Re-opening of the north sub-area on April 1 (day 91) initially attracted most of the fleet, but once again the fleet caught more *Illex* than *Loligo* on day 91(Figure 4). Around the same time catches were strong in the south, and most of the fleet returned south the next day. Fishing effort was not taken to the north again until April 5 and then produced a spike in CPUE on April 6 (day 96) (Figure 5), when 5 vessels caught 223 tonnes *Loligo* (Figure 4). Day 96 is considered the start of the second depletion north. The estimated prior for initial abundance was:

$$
\begin{aligned}
{}_{\text{predicted}}\,N_{N\ day\ 95} &= N_{N\ day\ 65} \times e^{-M \times (day\ 95 - day\ 65)} - CNMD_{N\ day\ 95} \\
&= 0.247 \times 10^{9} \times e^{-M \times (day\ 95 - day\ 65)} - 0.082 \times 10^{9} \\
&= 0.084 \times 10^{9}
\end{aligned}
$$

$$ {}_{\text{prior}}N_{\text{N day 96}} = {}_{\text{predicted}}N_{\text{N day 95}} \times \frac{\text{CPUE}_{\text{N day 96}}}{\text{CPUE}_{\text{N day 95}}} \Big/ \frac{\text{avg. Wt}_{\text{N day 96}}}{\text{avg. Wt}_{\text{N day 95}}} $$

$$ = 0.084 \times 10^9 \times 2.462 \ / \ 1.089 = 0.190 \times 10^9 \quad \textbf{(10)} $$

The prior distribution is shown as a red line on Figure 10, with maximum likelihood at ${}_{\text{prior}}N_{\text{N day 96}}$. The maximum likelihood of the depletion model, using equations (7, 8) was found at ${}_{\text{depletion}}N_{\text{N day 96}} = 0.177 \times 10^9$ (Figure 10, blue line). The distribution of the MCMC for this depletion period (Figure 10, gray bars) was anomalous in that it did not represent an average or intermediate between the prior and depletion model; having a modal likelihood lower than either. Due to the abrupt decrease of CPUE following day 96 (Figure 5), this depletion curve was relatively difficult to fit. In particular the relationship between the free parameters N and q_{avg} was asymptotic at low values of N; i.e., almost any value of q_{avg} showed high likelihood at low values of N. As a result, low values of N were over-accepted in the MCMC. This was partially remedied by restricting q_{avg} to ≤1.5× its optimized value, but the modal likelihood of the MCMC (approximately 0.130×10^9) still came out clearly lower than the maximum likelihood of the posterior (${}_{\text{post}}N_{\text{N day 96}} = 0.166 \times 10^9$).

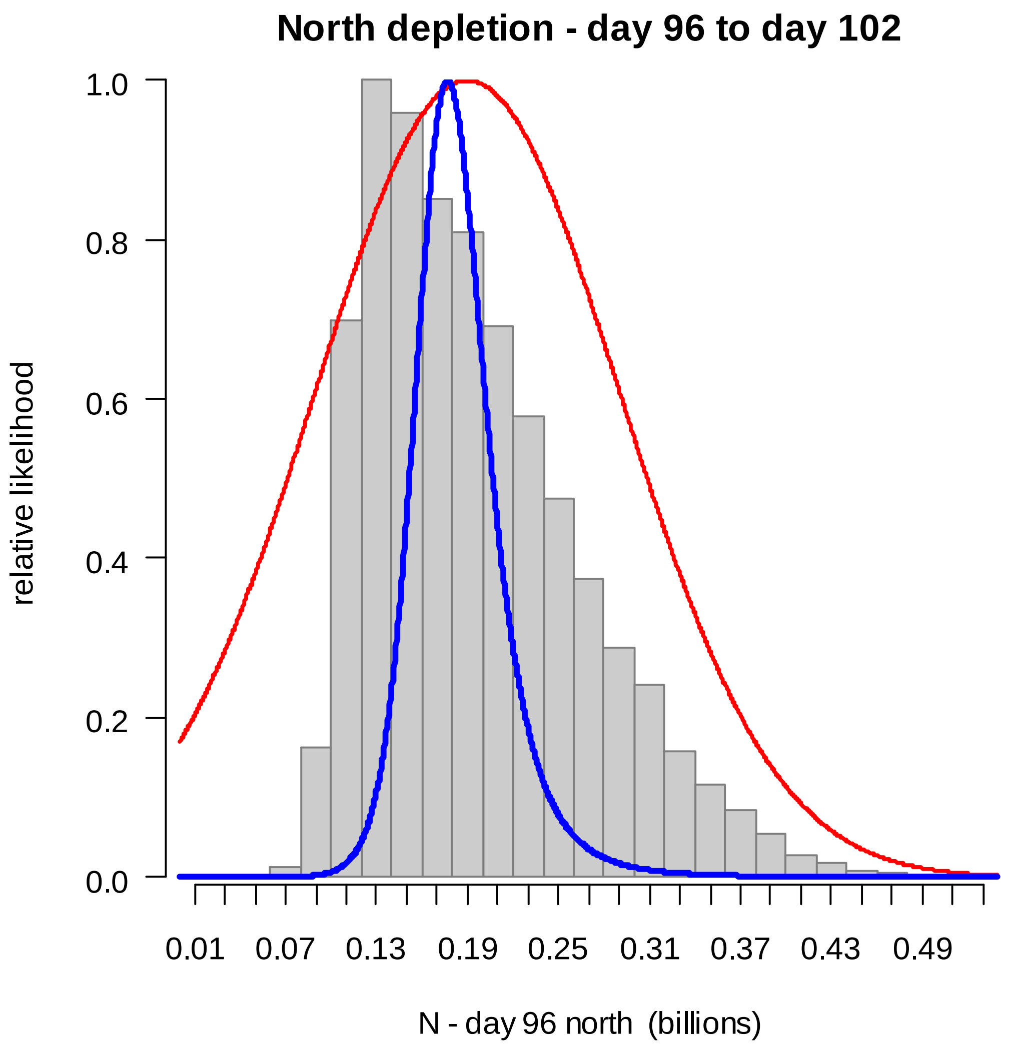

Figure 10 [previous page]. Model likelihood distributions for N billion *Loligo* present in the north sub-area fishery on day 96 (April 6). Red line: prior model (from CPUE ratio over previous day), blue line: depletion model from day 96 to day 102, gray bars: posterior.

First depletion south

For the first depletion south assumed to start on day 84, the estimated prior for initial abundance, using equations (3S, 4, 5), was:

$$
\begin{aligned}
CNMD_{S\text{ day }84} &= 0.026 \times 10^9 \\
{}_{\text{prior}}\,N_{S\text{ day }84} &= 0.197 \times 10^9 \times e^{-0.0133 \times (84-55)} - CNMD_{S\text{ day }84} \\
&= 0.108 \times 10^9 \qquad \textbf{(11)}
\end{aligned}
$$

The distribution of this prior is shown as the red line in Figure 11. The maximum likelihood of the depletion model, using equations (7, 8) was found at ${}_{\text{depletion}}\,N_{S\text{ day }84} = 0.099 \times 10^9$ (Figure 11, blue line). The maximum likelihood of the prior and the depletion model were thus close, with the maximum likelihood of the MCMC somewhat lower at ${}_{\text{post}}\,N_{S\text{ day }84} = 0.090 \times 10^9$ and accurately represented by the MCMC distribution (Figure 11, gray bars).

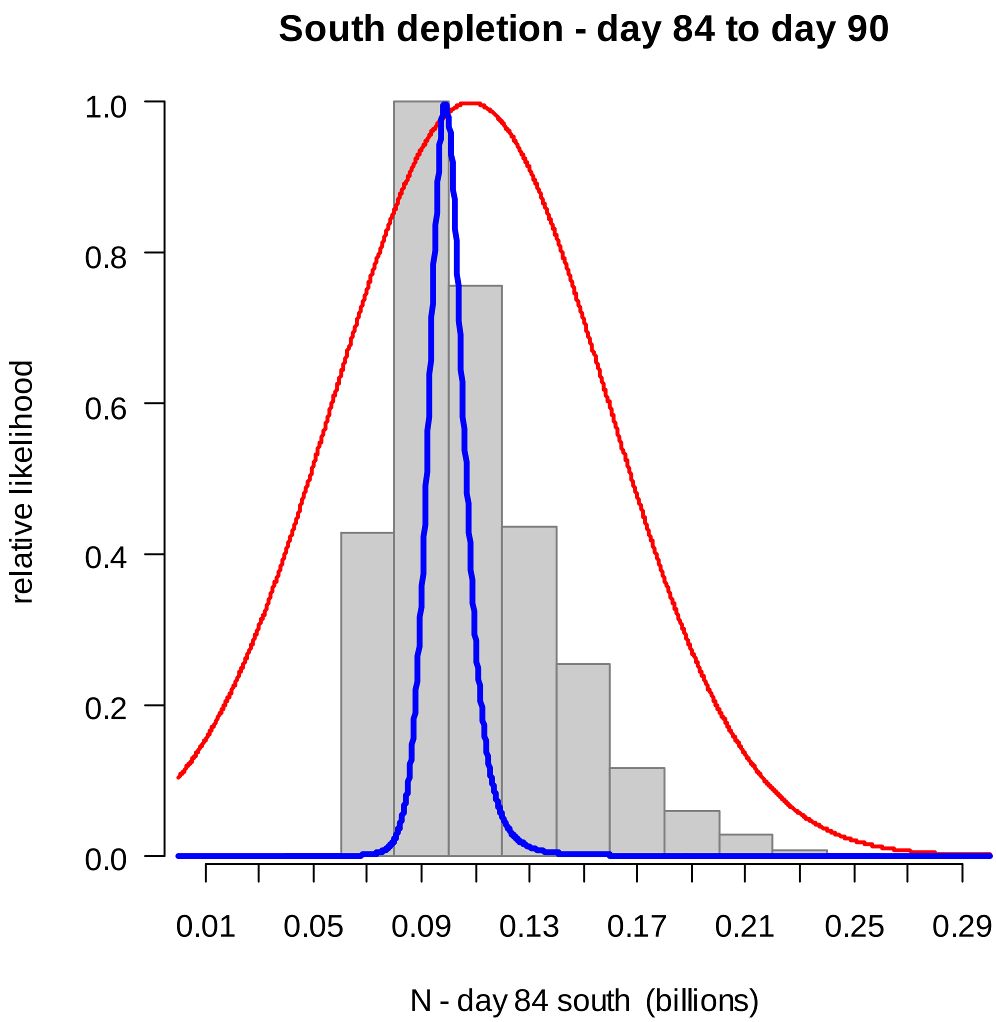

Figure 11 [previous page]. Model likelihood distributions for N billion *Loligo* present in the south sub-area fishery on day 84 (March 25). Red line: prior model (derived from pre-season survey data), blue line: depletion model from day 84 to day 90, gray bars: posterior.

Second depletion south

The second depletion south was identified on the day that fishing was re-opened in the north (April 1 - day 91), and the large change in CPUE south on day 91 may be due partially to the rapid shift in effort. However, observer data on *Loligo* in the south also changed noticeably before and after day 91 (Figures 6A and 6C) and it is therefore indicated that a new immigration had occurred at that time. The estimated prior for initial abundance was:

$$
\begin{aligned}
{}_{\text{predicted}}\,N_{\text{S day 90}} &= N_{\text{S day 84}} \times e^{-M \times (\text{day 90} - \text{day 84})} - \text{CNMD}_{\text{S day 90}} \\
&= 0.090 \times 10^9 \times e^{-M \times (\text{day 90} - \text{day 84})} - 0.044 \times 10^9 \\
&= 0.039 \times 10^9 \\
{}_{\text{prior}}\,N_{\text{S day 91}} &= {}_{\text{predicted}}\,N_{\text{S day 90}} \times \frac{\text{CPUE}_{\text{S day 91}}}{\text{CPUE}_{\text{S day 90}}} \,/\, \frac{\text{avg. Wt}_{\text{S day 91}}}{\text{avg. Wt}_{\text{S day 90}}} \\
&= 0.039 \times 10^9 \times 3.038 \,/\, 0.941 = 0.127 \times 10^9 \qquad \textbf{(12)}
\end{aligned}
$$

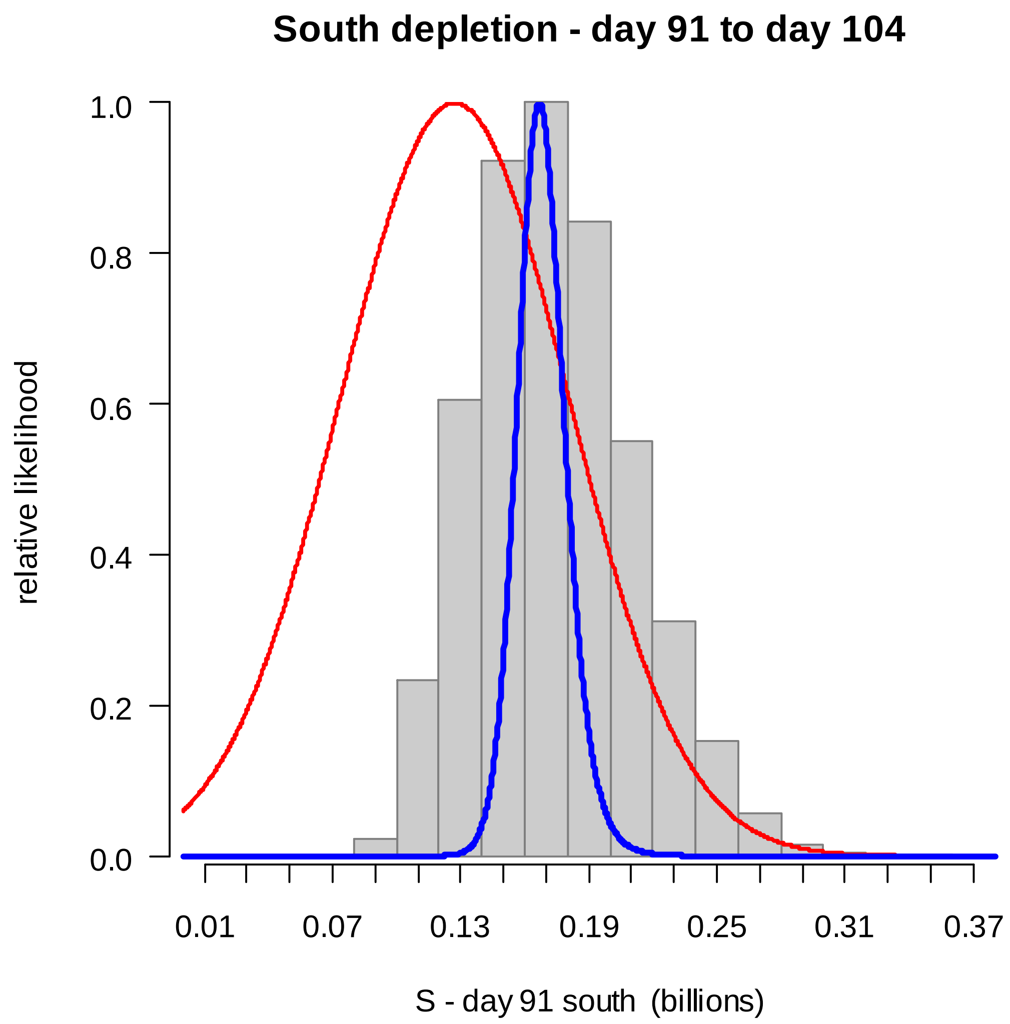

Figure 12 [previous page]. Model likelihood distributions for N billion *Loligo* present in the south sub-area fishery on day 91 (April 1). Red line: prior model (derived from pre-season survey data), blue line: depletion model from day 91 to day 104, gray bars: posterior.

The distribution of this prior is shown as the red line in Figure 12. The maximum likelihood of the depletion model, using equations (7, 8) was found at $_{depletion}\,N_{S\ day\ 91} = 0.167 \times 10^9$ (Figure 12, blue line). Maximum likelihood of the posterior was slightly higher at 0.173×10^9, which was accurately reflected by the mode of the MCMC (Figure 12, gray bars).

Escapement biomass

Escapement biomass was estimated from the number of *Loligo* in the fishing area at the end of the season (day 104; April 14) multiplied by the expected individual weight of *Loligo* on day 104. Calculations were made separately by north and south sub-areas, then summed.

Numbers of *Loligo* on day 104 were calculated according to equations (4, 5) whereby $N_{day\ 55}$ was replaced by the maximum likelihood $N_{start\ day}$ posterior of the last depletion, in either sub-area. Expected individual weights on day 104 were calculated from a generalized linear model (GLM) of daily average individual weight vs. day count for the period of either last depletion; up to and including day 104.

For the north sub-area:

$$\begin{aligned} N_{N\ day\ 104} &= {}_{post}N_{N\ day\ 96} \times e^{-M \times (day\ 104 - day\ 96)} - CNMD_{N\ day\ 104} \\ &= 0.166 \times 10^9 \times e^{-0.0133 \times 8} - 0.016 \times 10^9 \\ &= 0.133 \times 10^9 \\ B_{N\ day\ 104} &= 0.133 \times 10^9 \times 0.033\ \text{kg} = 4351.9\ \text{tonnes} \end{aligned} \qquad \textbf{(13)}$$

For the south sub-area:

$$\begin{aligned} N_{S\ day\ 104} &= {}_{post}N_{S\ day\ 91} \times e^{-M \times (day\ 104 - day\ 91)} - CNMD_{S\ day\ 104} \\ &= 0.173 \times 10^9 \times e^{-0.0133 \times 13} - 0.050 \times 10^9 \\ &= 0.096 \times 10^9 \\ B_{N\ day\ 104} &= 0.096 \times 10^9 \times 0.050\ \text{kg} = 4762.7\ \text{tonnes} \end{aligned} \qquad \textbf{(14)}$$

Error distributions for numbers of *Loligo* were obtained by replacing $N_{day\ 55}$ in equation 4 with values randomly drawn from the MCMC posterior distribution of the last depletion, instead of with the maximum likelihood posterior of the last depletion. Error distributions for individual weight were obtained by random-normal drawn values with mean equal to the GLM prediction, and standard error equal to the GLM standard error. Both random draws were simultaneously iterated 135,000× (5× the length of the MCMC) and multiplied together at each iteration. The resulting distributions, for north and south sub-area, were added together to estimate the total escapement biomass for the fishing area. This total distribution is shown in Figure 13. Maximum probability of the escapement biomass was 4,351.9 + 4,762.7 = 9,115 tonnes. Mean of the MCMC distribution was 10,066 tonnes, and 95% confidence interval [5735, 16026] tonnes. The risk analysis (Francis, 1991) of the fishery is defined as the proportion of the distribution below the escapement biomass limit of 10,000 tonnes. This risk was found equal to 53.5% (Figure 13). The distribution was thus right-skewed; slightly more than half the MCMC samples were below 10,000 tonnes but those above 10,000 tonnes were relatively further from the median.

The CPUE trends (Figure 5) and *Loligo* data (Figure 6) suggest that new immigrations / depletions may have been starting in the final days of the season, both north and south. In particular, the last three days' catches in the south were poorly fit by the depletion curve extending back from day 91 (Figure 8). However, new immigrations could no longer be modelled with meaningful precision over those last 2-3 days.

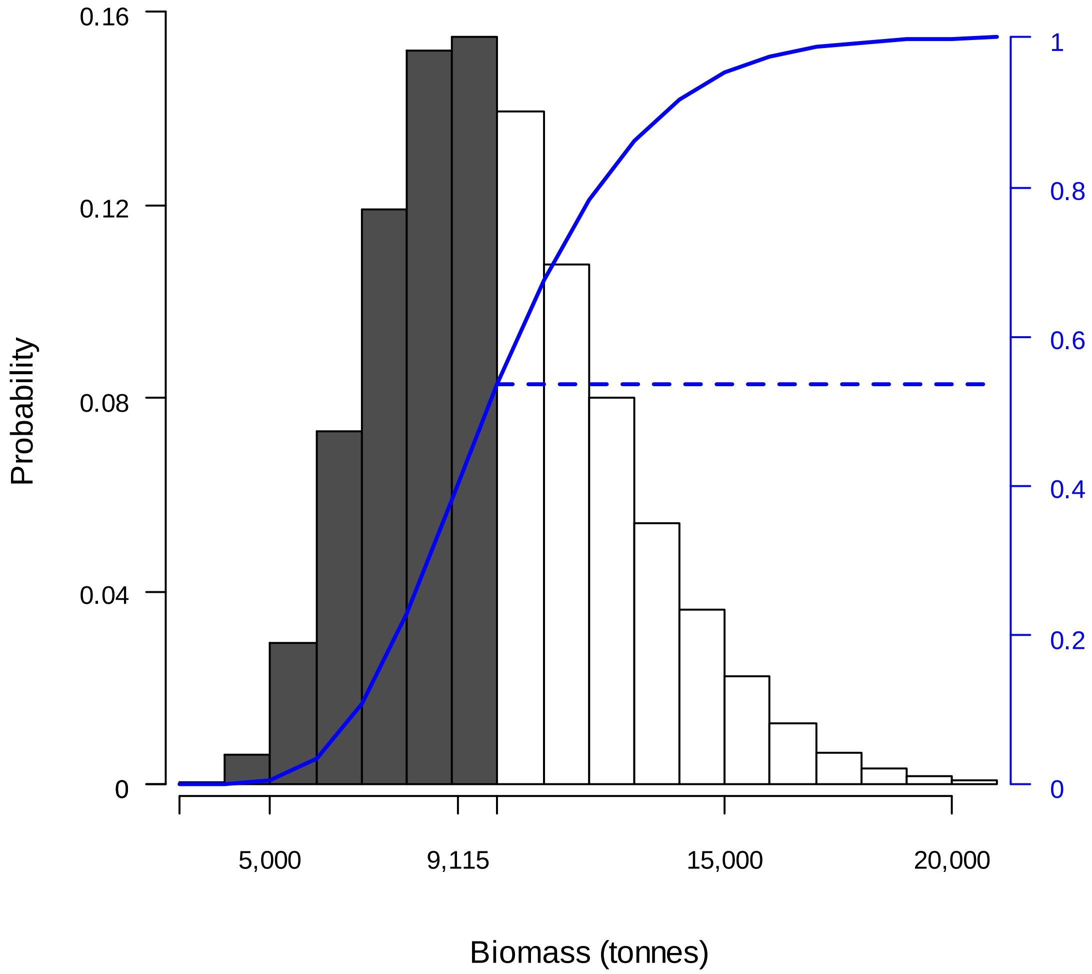

Figure 13. Probability distribution of *Loligo* biomass at the end of the season, April 14. Distribution samples less than the biomass escapement limit of 10,000 tonnes are shaded dark gray. Cumulative probability is shown as a solid blue curve. The broken blue line indicates that the probability of less than 10,000 tonnes escapement biomass was 53.5%.

Immigration and catch rate

Total *Loligo* immigration was inferred as the difference between the posterior estimate on each depletion start day (when the immigrations putatively occurred) and the predicted number on that day that would be accounted for by depletion of the preceding estimated biomass alone. Error distributions were determined from the MCMCs and from day-to-day changes in average individual *Loligo* weight. The first depletions north and south were not considered new immigration days. For the second depletion north; start day 96:

$$_{post}N_{N\ day\ 96} = 0.166 \times 10^9 \pm 74.4\% \quad = \quad 0.166 \pm 0.123 \times 10^9$$

$$\begin{aligned} _{predicted}N_{N\ day\ 96} &= N_{N\ day\ 65} \times e^{-M \times (day\ 96 - day\ 65)} - CNMD_{N\ day\ 96} \\ &= 0.247 \times 10^9 \times e^{-M \times (day\ 96 - day\ 65)} - 0.082 \times 10^9 \\ &= 0.081 \times 10^9 \pm 12.9\% \quad = \quad 0.081 \pm 0.010 \times 10^9 \end{aligned}$$

$$\begin{aligned} _{immigration}N_{N\ day\ 96} &= (0.166 - 0.081) \pm \sqrt{0.123^2 + 0.010^2} \times 10^9 \\ &= 0.084 \pm 0.124 \times 10^9. \end{aligned}$$

$$avg.Wt_{N\ day\ 96} = 0.054\ kg \pm 17.2\%$$

$$\begin{aligned} _{immigration}B_{N\ day\ 96} &= 0.084 \times 10^9 \times 0.054/1000 \pm \sqrt{\left(\frac{0.124}{0.084}\right)^2 + 0.172^2} \\ &= 4512.1 \pm 6666.6\ tonnes \end{aligned} \qquad \textbf{(15)}$$

For the second depletion south; start day 91:

$$_{post}N_{S\ day\ 91} = 0.173 \times 10^9 \pm 21.7\% \quad = \quad 0.173 \pm 0.038 \times 10^9$$

$$\begin{aligned} _{predicted}N_{S\ day\ 91} &= N_{S\ day\ 84} \times e^{-M \times (day\ 91 - day\ 84)} - CNMD_{S\ day\ 91} \\ &= 0.090 \times 10^9 \times e^{-M \times (day\ 91 - day\ 84)} - 0.047 \times 10^9 \\ &= 0.035 \times 10^9 \pm 39.7\% \quad = \quad 0.035 \pm 0.014 \times 10^9 \end{aligned}$$

$$\begin{aligned} _{immigration}N_{S\ day\ 91} &= (0.173 - 0.035) \pm \sqrt{0.038^2 + 0.014^2} \times 10^9 \\ &= 0.138 \pm 0.040 \times 10^9. \end{aligned}$$

$$avg.Wt_{S\ day\ 91} = 0.043\ kg \pm 5.4\%$$

$$\begin{aligned} _{immigration}B_{S\ day\ 91} &= 0.138 \times 10^9 \times 0.043/1000 \pm \sqrt{\left(\frac{0.040}{0.138}\right)^2 + 0.054^2} \\ &= 5903.0 \pm 1748.7\ tonnes \end{aligned} \qquad \textbf{(16)}$$

The total estimated immigration biomass was thus:

$$\begin{aligned} _{immigration}B_{total} &= 4512.1 + 5903.0 \pm \sqrt{6666.6^2 + 1748.7^2} \\ &= 10{,}415 \pm 6{,}892\ tonnes \end{aligned} \qquad \textbf{(17)}$$

And the estimated total biomass (initial + immigration; equation 2 + equation 17) to have been present in the Falkland Islands *Loligo* Box fishery zone in the first season of 2011 was:

$$16{,}095 \pm 8{,}263 + 10{,}415 \pm 6{,}892 \quad = \quad 26{,}510 \pm 10{,}760\ tonnes \qquad \textbf{(18)}$$

Giving a total catch rate of:

$$15{,}271 / 26{,}510 \pm 10{,}760\ tonnes \quad = \quad 57.6\% \pm 40.6\% \qquad \textbf{(19)}$$

References

Agnew, D.J., Baranowski, R., Beddington, J.R., des Clers, S., Nolan, C.P. 1998. Approaches to assessing stocks of *Loligo gahi* around the Falkland Islands. Fisheries Research 35:155-169.

Arkhipkin, A.I., Grzebielec, R., Sirota, A.M., Remeslo, A.V., Polishchuk, I.A., Middleton, D.A. 2004a. The influence of seasonal environmental changes on ontogenetic migrations of the squid *Loligo gahi* on the Falkland shelf. Fisheries Oceanography 13:1-9.

Arkhipkin, A.I., Middleton, D.A.J., Sirota, A.M., Grzebielec, R. 2004b. The effect of Falkland Current inflows on offshore ontogenetic migrations of the squid *Loligo gahi* on the southern shelf of the Falkland Islands. Estuarine, Coastal, and Shelf Science 60:11-22.

Arkhipkin, A.I., Middleton, D.A.J. 2002a. Inverse patterns in abundance of *Illex argentinus* and *Loligo gahi* in Falkland waters: possible interspecific competition between squid? Fisheries Research 59:181-196.

Arkhipkin, A.I., Middleton, D.A.J. 2002b. Sexual segregation in ontogenetic migration by the squid *Loligo gahi* around the Falkland Islands. Bulletin of Marine Science 71:109-127.

Arkhipkin, A.I., Middleton, D.A.J., Barton, J. 2008. Management and conservation of a short-lived fishery resource: *Loligo gahi* around the Falkland Islands. American Fisheries Society Symposium 49:1243-1252.

Arreguin-Sanchez, F. 1996. Catchability: a key parameter for fish stock assessment. Reviews in Fish Biology and Fisheries 6:221-242.

Barton, J. 2002. Fisheries and fisheries management in Falkland Islands Conservation Zones. Aquatic Conservation: Marine and Freshwater Ecosystems 12:127-135.

Brooks, S.P., Gelman, A. 1998. General methods for monitoring convergence of iterative simulations. Journal of computational and graphical statistics 7:434-455.

DeLury, D.B. 1947. On the estimation of biological populations. Biometrics 3:145-167.

Efron, B. 1981. Nonparametric estimates of standard error: the jackknife, the bootstrap and other methods. Biometrika 68:589-599.

Francis, R.I.C.C. 1991. Risk analysis in fishery management. NAFO Scientific Council Studies 16:143-148.

Gamerman, D., Lopes, H.F. 2006. Markov Chain Monte Carlo. Stochastic simulation for Bayesian inference. 2nd edition. Chapman & Hall/CRC.

Haimovici, M., Brunetti, N., Rodhouse, P.G., Csirke, J., Leta, R.H. 1998. *Illex argentinus*. In: Rodhouse, P.G., Dawe, E.G., O'Dor, R.K. (Eds.), Squid Recruitment Dynamics. The Genus Illex as a Model, the Commercial Illex Species and Influences on Variability. FAO Fisheries Technical Paper, Vol. 376. FAO, Rome, pp. 27–58.

Harte, M., Barton, J. 2007. Balancing local ownership with foreign investment in a small island fishery. Ocean and Coastal Management 50:523-537.

Patterson, K.R. 1988. Life history of Patagonian squid *Loligo gahi* and growth parameter estimates using least-squares fits to linear and von Bertalanffy models. Marine Ecology Progress Series 47:65-74.

Payá, I. 2006. Fishery Report. *Loligo gahi*, Second Season 2006. Fishery statistics, biological trends, stock assessment and risk analysis. Technical Document, Falkland Islands Fisheries Department.

Payá, I. 2009. Fishery Report. *Loligo gahi*, First Season 2009. Fishery statistics, biological trends, stock assessment and risk analysis. Technical Document, Falkland Islands Fisheries Department.

Payá, I. 2010. Fishery Report. *Loligo gahi*, Second Season 2009. Fishery statistics, biological trends, stock assessment and risk analysis. Technical Document, Falkland Islands Fisheries Department.

Punt, A.E., Hilborn, R. 1997. Fisheries stock assessment and decision analysis: the Bayesian approach. Reviews in Fish Biology and Fisheries 7:35-63.

Roa-Ureta, R., Arkhipkin, A.I. 2007. Short-term stock assessment of *Loligo gahi* at the Falkland Islands: sequential use of stochastic biomass projection and stock depletion models. ICES Journal of Marine Science 64:3-17.

Rosenberg, A.A., Kirkwood, G.P., Crombie, J.A., Beddington, J.R. 1990. The assessment of stocks of annual squid species. Fisheries Research 8:335-350.

Winter, A. 2010a. *Loligo gahi* stock assessment, first season 2010. Technical Document, Falkland Islands Fisheries Department.

Winter, A. 2010b. *Loligo gahi* stock assessment, second season 2010. Technical Document, Falkland Islands Fisheries Department.

Winter, A., Davidson, D., Watson, M. 2011. *Loligo gahi* stock assessment survey, first season 2011. Technical Document, Falkland Islands Fisheries Department.